Intracellular transport is accelerated in early apoptotic cells

Bo Li[a,b], Shuo-Xing Dou[a,b], Jing-Wen Yuan[a,b], Yu-Ru Liu[a], Wei Li[a], Fangfu Ye[a,b], Peng-Ye Wang[a,b], and Hui Li[a,1]

[a]Key Laboratory of Soft Matter Physics, Beijing National Laboratory for Condensed Matter Physics, Institute of Physics, Chinese Academy of Sciences, Beijing 100190, China; and [b]School of Physical Sciences, University of Chinese Academy of Sciences, Beijing 100049, China

Edited by David A. Weitz, Harvard University, Cambridge, MA, and approved October 22, 2018 (received for review June 11, 2018)

Intracellular transport of cellular proteins and organelles is critical for establishing and maintaining intracellular organization and cell physiology. Apoptosis is a process of programmed cell death with dramatic changes in cell morphology and organization, during which signaling molecules are transported between different organelles within the cells. However, how the intracellular transport changes in cells undergoing apoptosis remains unknown. Here, we study the dynamics of intracellular transport by using the single-particle tracking method and find that both directed and diffusive motions of endocytic vesicles are accelerated in early apoptotic cells. With careful elimination of other factors involved in the intracellular transport, the reason for the acceleration is attributed to the elevation of adenosine triphosphate (ATP) concentration. More importantly, we show that the accelerated intracellular transport is critical for apoptosis, and apoptosis is delayed when the dynamics of intracellular transport is regulated back to the normal level. Our results demonstrate the important role of transport dynamics in apoptosis and shed light on the apoptosis mechanism from a physical perspective.

apoptosis | intracellular dynamics | single-particle tracking

Apoptosis is a finely regulated form of programmed cell death that plays key roles in many biological processes, such as embryonic and tissue development, and homeostasis in multicellular organisms (1). Deregulation of apoptosis can lead to an accumulation of unwanted cells and result in the development of a tumor (2). Apoptosis is not only controlled by a complicated signaling pathway but also undergoes a highly dynamic transformation. The most notable feature of apoptosis is the change of cell morphology: cell shrinkage, nuclear condensation, blebbing, and the formation of apoptotic bodies (3). These mass-scale transformations take place in the late phase of apoptosis, when caspase family members begin to cleave intracellular proteins and demolish cell structures (4). Recently, with the aid of new imaging technologies, studies have revealed detailed information about the transformations of macromolecules and reorganizations of organelles in late apoptotic cells (5, 6). In early apoptosis, however, there is no mass-scale transformation in the cellular structure, but numerous signaling molecules are transported within the cell environment as they are required in preparation for apoptosis (7). While the transformations in macromolecules and structures of late apoptotic cells have been well studied, the dynamics of intracellular transport in early apoptotic cells still remain unclear.

Intracellular transport is the critical way to deliver different cargos, such as molecules, vesicles, and other organelles, in the crowded cytoplasm to maintain normal cell physiology (8). In the process of cell apoptosis, the intracellular transport of proteins, especially those participating in the apoptotic signaling pathway, is crucial for its initiation. For example, certain caspases are translocated from the cytoplasm into mitochondria or the nucleus (7); cytochrome *c* is released from the mitochondrial intermembrane space to the cytoplasm, which is also a marker of early apoptosis (9). For these dynamic changes of molecule distribution to occur within early apoptotic cells, the intracellular transport dynamics, which acts as the physical basis, is indispensable. Characterization of the intracellular dynamics is thus essential for understanding the related biological processes and their physical environments in apoptotic cells.

Moreover, as the occurrence of apoptosis is asynchronous in individual cells (10), previous studies of apoptosis in a cell population, which generally give the averaged results, have not been sensitive and accurate enough to detect the subtle changes in cells at a specific apoptotic stage. The desirable way for observing the intracellular transport in early apoptotic cells is to use the single-particle tracking (SPT) method combined with some single-cell apoptosis detection technique under a microscope. SPT provides direct dynamical information about individual molecules, vesicles, and organelles with nanometer spatial and millisecond temporal resolutions, which is not available to ensemble average methods such as fluorescence recovery after photobleaching (11). Note, however, that how to identify those adherent cells that are at the early stage of apoptosis under the microscope is challenging, since there is no reliable change in the morphology of a cell at this stage, while it is not known whether the present fluorescence markers applied to flow cytometry can be effective for single-cell detection of early apoptosis (12).

In the present work, we use the SPT method to directly study the intracellular transport of endocytic vesicles in early apoptotic cells. The trafficking of endocytic vesicles is one of the best-characterized models for studying intracellular transport. With the successful identification of early apoptotic cells by an indicator tetramethylrhodamine ethyl ester (TMRE) (12), we observe that, remarkably, the directed transport is accelerated when cells are entering

Significance

Apoptosis is a programmed cell death and critical to embryonic development, organism homeostasis, and even cancer. Although the biological aspects of apoptosis such as the molecular signaling pathway and cellular structure transformation have been intensively studied over the past 40 years, studies of the physical aspects such as intracellular dynamics are still lacking. We report that the intracellular transport with both directed and nondirected motions is accelerated in early apoptotic cells, and this results from an elevated cytosolic ATP level. Furthermore, we find that, by regulating the accelerated intracellular transport back to the normal level, the apoptotic progress is significantly delayed. This study, from the physical perspective, highlights the critical importance of intracellular transport dynamics in apoptosis.

Author contributions: P.-Y.W. and H.L. designed research; B.L., J.-W.Y., and H.L. performed research; Y.-R.L., W.L., and F.Y. contributed new reagents/analytic tools; B.L., S.-X.D., P.-Y.W., and H.L. analyzed data; and B.L., S.-X.D., P.-Y.W., and H.L. wrote the paper.

The authors declare no conflict of interest.

This article is a PNAS Direct Submission.

[1]To whom correspondence should be addressed. Email: huili@iphy.ac.cn.

This article contains supporting information online at www.pnas.org/lookup/suppl/doi:10.1073/pnas.1810017115/-/DCSupplemental.

apoptosis. By examining several factors involved in the intracellular dynamics, we find out that the acceleration of intracellular directed motion results from an elevated adenosine triphosphate (ATP) concentration in the cells. In addition, for the same reason, the diffusive motion, which results from intracellular fluctuations driven by random motor activities, is also enhanced. Furthermore, we observe that the apoptotic process would be delayed if the activity of intracellular transport is decreased to the normal level, through applying an external osmotic pressure to the cells. These results suggest that the enhancement of intracellular dynamics plays an important role in the apoptotic process, at least at the early stage.

Results

First, to directly measure the dynamics of directed transport, we monitor the endocytic trafficking of the epidermal growth factor receptor (EGFR) in living cells by using the SPT method. EGFR is a transmembrane protein, and its endocytic trafficking has been well studied (13). EGFR molecules on the cell membrane are labeled by biotin-EGF and streptavidin–quantum dot (QD) at 4 °C consecutively, and then, after the temperature is elevated to 37 °C, the endocytosis of EGFR–EGF-QD complexes begins [as commonly done before (14, 15)]. Continuous imaging of the intracellular transport of QD-labeled endocytic vesicles is performed at a speed of 10 Hz, within a time period from 20 to 40 min after the start of endocytosis (Fig. 1*A*). The focal plane is always fixed at 1.5 μm above the glass surface. From the trajectories of these vesicles extracted from the movies, two kinds of intracellular transport in the cells could be classified according to the motion type: directed motion and nondirected diffusive motion. The former is driven by motor proteins coherently along specific cytoskeleton structures (8), whereas the latter is by randomly fluctuating forces due to stochastic motor activities and thus different from the traditional thermal motion (16–18). We apply an automatic algorithm to identify and extract the segments of directed motion from the whole trajectories. As shown in Fig. 1 *B* and *C*, a moving window of 20 points is used to determine the local dynamic parameters along each trajectory, including the exponent α indicating the nonlinear relationship of mean square displacement (MSD) with time and the directional persistence <cosβ>, in which β indicates the angle between adjacent steps (15, 19). Then the segments of directed motion from the trajectory are determined based on the above two parameters (*Materials and Methods*). To demonstrate the effectiveness of our identification algorithm, we apply nocodazole (NOC) to disrupt the microtubules in the cells. In this case, almost no segment of directed motion could be detected (Fig. 1*D*), just as expected, because directed motions of vesicles are along microtubules after endocytosis (15, 20). Note that there is no difference in the intracellular transport dynamics observed within different cell layers (*SI Appendix*, Fig. S1), indicating that our result obtained from one cell layer could represent that for the whole cell.

Then we start to investigate the intracellular transport in early apoptotic cells. We use 50 μM cisplatin to treat the cells for 12 h before introducing the apoptosis. Cisplatin is a well-known DNA-targeted drug and commonly used for testicular, ovarian, as well as non–small-cell lung cancers (21). It is known that apoptotic progress induced by stimuli is not synchronous at the single-cell level but happens stochastically within a time range (10). Therefore, it is critical to identify the early apoptotic cells in the heterogeneous cell population. Different from cells in the late stage of apoptosis, early apoptotic cells remain spread out and in good attachment to the coverslip surface, just as normal ones; thus, this feature cannot be used for their identification. We first try using Annexin V, a common apoptosis probe in flow cytometry, to detect the exposure of plasma membrane inner phosphatidyl serine (PS) (22). However, we find that Annexin V staining is not sensitive enough to detect early apoptotic cells under the microscope. The cells cannot be stained until shrinking and blebbing (*SI*

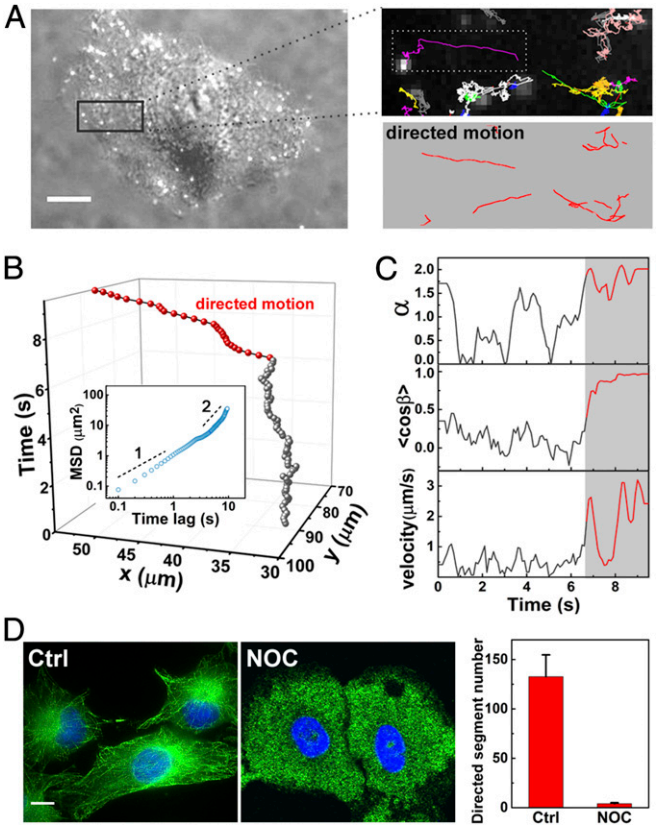

Fig. 1. Dynamic analysis of intracellular transport by tracking QD-labeled endocytic vesicles. (*A*) Florescent image of QDs overlaid with bright-field image of an A549 cell (*Left*). EGF-QDs are internalized into cells rapidly after binding to the surface EGFRs. The *Right Upper* panel shows the trajectories of QDs in the rectangular region of the left panel. The *Right Lower* panel shows segments of directed motion extracted automatically from the above trajectories by the algorithm. (*B*) Position of a QD-labeled vesicle as a function of time, with a temporal resolution of 100 ms. The trajectory is segmented into directed motion (red) and diffusive motion (gray). (*Inset*) MSD of the trajectory and approximate power-law slopes of 1 and 2 are indicated. (*C*) Temporal exponent α, directional persistence <cosβ>, and velocity for each point in the trajectory in *B*. α denotes the nonlinear relationship of MSD with time, and β represents the angle between adjacent steps along the trajectory. The red parts correspond to the period of directed motion and the gray ones to diffusive motion. The window size for temporal MSD analysis is 20 points. (*D*) Nocodazole (NOC) treatment disrupts the microtubules (*Left*) and abolishes the directed motion of intracellular transport (*Right*). Cells are treated with 60 μM nocodazole for 30 min. Microtubules are labeled with rat anti-tubulin and Alexa 488 goat anti-rat IgG conjugate consecutively. The average numbers of segments in directed motion per cell are compared. Error bars indicate SEM. Ctrl, control. (Magnification: *A*, *Right*: 4×.) (Scale bar, 10 μm.)

Appendix, Fig. S2), consistent with a previous study showing that the inner PS exposure temporally associates with cell rounding and blebbing (23). Then, we try using another apoptosis indicator, TMRE, to probe the loss of mitochondrial membrane potential (MMP) by measuring the loss of TMRE signal (12). The loss of MMP is directly related to the release of cytochrome *c* and the activation of apoptosis (24). We find that the TMRE signal is obviously weaker in some of the cisplatin-treated cells, although their morphologies have no detectable changes as seen in the bright-field images (Fig. 2 *A* and *B*). This indicates that TMRE is more sensitive and suitable for the detection of adherent apoptotic cells. By labeling the nuclei with Hoechst, it can be observed that the nuclei are aberrant in these cells, consistent with the feature of early apoptosis (Fig. 2*A*). TMRE works well here, probably because the loss of MMP is ahead of the PS flip. We find

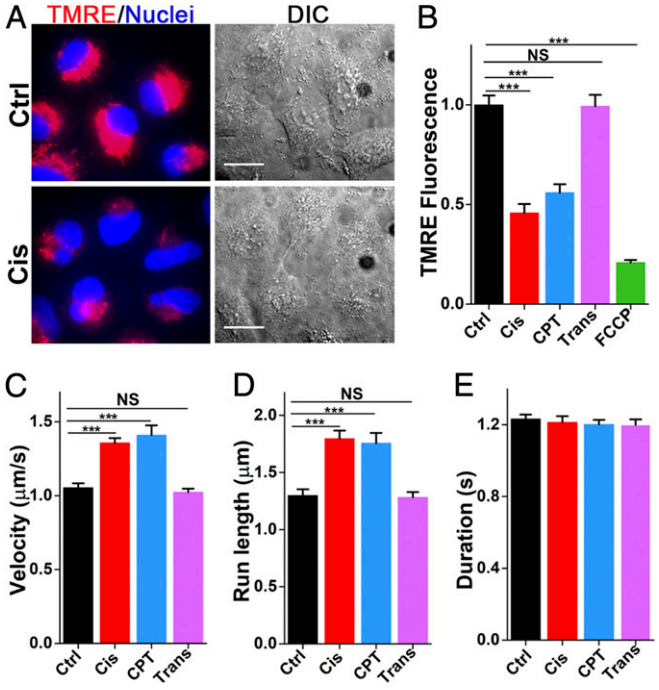

Fig. 2. Detection of early apoptotic cells under fluorescence microscopy. Directed motion is accelerated in early apoptotic cells. (*A*) Merged images of TMRE (red) and nuclei (blue) for control and cisplatin-treated cells. Bright-field images of the cells are shown in the *Right* panels. Mitochondria and nuclei are labeled by 100 nM TMRE and Hoechst 33342 for 10 min, separately. Decrease of fluorescence intensity of TMRE indicates the loss of MMP, which is a marker for the early apoptosis. (Scale bar, 20 μm.) (*B*) Relative TMRE fluorescence intensities of single cells in control group and that treated with cisplatin, CPT, transplatin, and FCCP. (*C–E*) Average velocity, run length, and duration of directed motion in control, cisplatin-, CPT-, and transplatin-treated cells. A549 cells are incubated with 50 μM cisplatin for 12 h, 5 μM CPT for 24 h, 50 μM transplatin for 12 h, and 20 μM FCCP for 40 min, respectively. ***$P < 0.001$ (two-sample t test). Ctrl, control; NS, not significant. Error bars indicate SEM. See *SI Appendix*, Table S1 for detailed sample sizes.

that, among the cisplatin-treated cells, about 48.5% with normal morphology show obvious decrease in TMRE fluorescence intensity compared with the control cells, indicating their early stage of apoptosis. To further verify the ability of the TMRE approach to detect the loss of MMP, we apply carbonyl cyanide-4-(trifluoromethoxy) phenylhydrazone (FCCP) as a positive control to eliminate MMP (12). In this case, we observe the loss of TMRE signal (Fig. 2*B*). These results demonstrate that TMRE can be used to indicate early apoptotic cells in our experiments.

It has been shown that, besides apoptosis, cisplatin could also induce necrosis of cancer cells in a drug dosage-dependent manner (25, 26). The necrosis is also accompanied with the loss of MMP, which may not be differentiated from apoptosis with TMRE staining (27). In the following, we confirm the cells in our experiments are indeed in the early apoptotic state rather than in the early necrotic state with two pieces of evidence. First, when examining the cellular morphology, A549 cells treated by 50 μM cisplatin for 24 h show the characteristic shrinking and blebbing of late apoptotic cells. However, the characteristic cellular swelling of late necrotic cells appears when the concentration of cisplatin is increased to 2 mM. In addition, nuclear staining of propidium iodide (PI) indicates the perforation of plasma membrane, which is also a necrotic characteristic (*SI Appendix*, Fig. S3*A*). Second, we use the caspase inhibitor z-VAD(OMe)-FMK (zVAD) to prevent caspase activation, which is the critical step for apoptosis, but not for necrosis (28). Therefore, the population of dead cells in the presence of zVAD should solely come from necrotic cells. We find that cell death is almost completely inhibited by 100 μM zVAD when cells are treated with 50 μM cisplatin (*SI Appendix*, Fig. S3*B*), indicating that only apoptosis is induced by cisplatin at the low concentration in our experiments. However, there are populations of dead cells with treatment by 2 mM cisplatin, even with zVAD, indicating that besides apoptosis, necrosis is also induced with a high concentration of cisplatin (25).

With the early apoptotic cells identified, we explore the directed motion of intracellular transport in them by observing the movements of QD-labeled endocytic vesicles containing EGFRs. Interestingly, we find that the directed motion is significantly accelerated in these cisplatin-treated early apoptotic cells, with the mean velocity and run length increasing by 30% and 38%, respectively (Fig. 2 *C–E* and *SI Appendix*, Fig. S4). More detailed sample sizes and dynamical parameters are shown in *SI Appendix*, Table S1. It is generally known that the anticancer mechanism of cisplatin is that it prevents DNA replication and transcription by binding to chromatin DNA, and subsequently blocks the cell proliferation (29). Until now, there is no report of a correlation between cisplatin and intracellular directed motion. The above observed phenomenon is striking and unpredicted. Then we further validate the experimental observation by studying the movements of endocytic streptavidin–QDs or endocytic fluorescence microspheres (*SI Appendix*, Fig. S5). The results for the nonfunctional cargos are consistent with the above results for functional cargos, indicating the acceleration of directed motion in these cisplatin-treated early apoptotic cells is universal for the intracellular transport.

To determine whether the acceleration of directed motion is due to a direct impact of cisplatin on the motor-driven movements or, alternatively, to the common death-causing effect such as apoptosis, we use camptothecin (CPT), another standard apoptosis-inducing reagent, to induce apoptosis (30). The cell death is also inhibited in the presence of zVAD, eliminating the possibility of CPT-induced necrosis here (*SI Appendix*, Fig. S3*C*). Similar to the cisplatin-treated cells, the TMRE signal is observed to decrease in those CPT-treated cells that remain adhesive and spread out, indicating their early apoptosis state (Fig. 2*B*). In these cells, the directed motion of endocytic vesicles is also accelerated, with increased velocity and run length (Fig. 2 *C–E* and *SI Appendix*, Fig. S6), just as in the cisplatin-treated cells. The time duration of directed motion remains nearly the same, indicating that the affinity of motor proteins to the microtubules does not change in the two different experiments. From the whole trajectories, the MSD curves can be obtained (*SI Appendix*, Fig. S7). MSD increases more quickly for both cisplatin- and CPT-treated cells than for the control, consistent with the acceleration of directed motion.

To further exclude the possibility that the above observed acceleration could be due to a direct influence of cisplatin on motor-driven movements, such as through binding to the motor proteins or microtubules, we investigate the effect of transplatin on the directed motion. Transplatin is the transstereoisomer of cisplatin but has no pharmacological effect in blocking proliferation of cells (31). This makes transplatin an ideal parallel model for cisplatin in our experiments. As expected, both the dynamic parameters of directed motion and the TMRE level remain unchanged in transplatin-treated cells (Fig. 2). That is, transplatin has no influence on the directed motion even with the same leaving group as cisplatin, because it lacks the ability of apoptosis induction. These results demonstrate that the acceleration of directed motion of intracellular transport in cisplatin-treated cells is a physiological effect of early apoptosis.

To find out the cause of the acceleration of directed motion in early apoptotic cells, we investigate three key elements closely related to the directed motion: microtubules, motor proteins, and endocytic vesicles (8). First, we check the microtubules under different conditions and see no obvious change in their distribution and morphology in immunofluorescence images (*SI Appendix*, Fig. S8*A*). Since the directed movements are along

microtubules, we measure the curvatures of segments of directed motion. The bending degrees for the different groups are similar (*SI Appendix*, Fig. S8 *B* and *C*), indicating that the microtubule shape or the bending degree of runs are not involved in the acceleration. Second, we check the density of motor protein dyneins, which mainly transport cargos from the microtubule plus end at the cell periphery to the minus end at the cell center (8). We find there is no difference in the density or distribution of dyneins between the control and cisplatin-treated cells, as shown in *SI Appendix*, Fig. S9 *A* and *B*. Third, we check the endocytic vesicles. From our previous study, the endocytic vesicles are mainly early endosomes in the first 30 min after endocytosis, and then transferred to lysosomes (13, 15). However, no obvious difference in the distribution and morphology of early endosomes and lysosomes could be seen between the control and cisplatin-treated cells (*SI Appendix*, Fig. S10). All of the above results suggest that these three factors that directly correlate with the directed motion play no roles in the acceleration of directed movements. As a direct impact on motor-driven movements from cisplatin is excluded, certain indirect effects from the apoptosis should contribute to the increase of velocity.

It is well known that apoptosis is a precisely controlled and energy-dependent process (32). Intracellular ATP is critical for apoptosis, and for motor proteins as their energy source. Thus, we try to find out whether the acceleration of directed motion is related to the cytosolic ATP concentration. A conventional luciferase assay is used to measure the total ATP content in cell lysates. After considering the variations in cell density under different drug treatments, we compare the relative amounts of ATP under different conditions and find that the cytosolic ATP concentrations in cisplatin- and CPT-treated cells are increased by 33% and 49%, respectively, compared with that in the control cells (Fig. 3*A*). For the transplatin-treated cells, no change is observed. The elevated ATP level is very likely the cause of the accelerated directed motion, since the velocities of microtubule-associated motor proteins such as dyneins and kinesins are reported to increase with increasing ATP concentration in experiments (33). The elevation of intracellular ATP level has been observed in apoptotic cells before, which is suggested to be a requisite for apoptosis (34). Note that it has also been shown before that the total cellular ATP level is reduced or remains unchanged during apoptosis (35, 36), but we think it may be underestimated due to the drop in the viable cell number in the apoptosis group, in which cell proliferation is inhibited. Indeed, we check the cell number for each condition right before the test of ATP level, and find that the cell densities of cisplatin- and CTP-treated cells decrease by 28% and 38%, respectively, compared with the control. The reason for the elevated ATP level is probably that, as the mitochondrial function is affected during apoptosis (37), the glycolytic reaction is likely to be enhanced to supply more ATP (34).

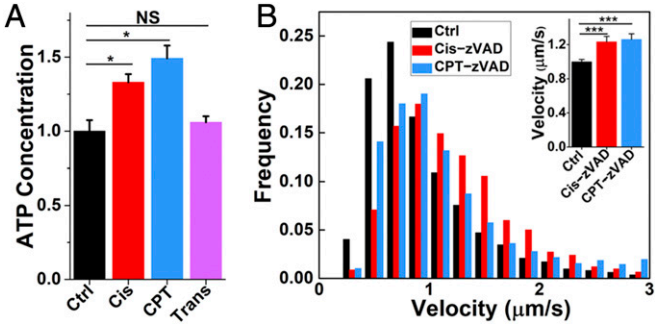

Fig. 3. Increase of cytosolic ATP in early apoptotic cells. (*A*) Normalized cytosolic ATP levels in control and drug-treated A549 cells. Cells are treated with 50 μM cisplatin for 12 h, 50 μM transplatin for 12 h, and 5 μM CPT for 24 h, respectively, before measurements. Data are averaged from four independent experiments. $*P < 0.05$ (two-sample *t* test). Ctrl, control; NS, not significant. Error bars indicate SD. (*B*) Comparison of the distributions of velocity of directed motion in control cells, and that treated with cisplatin-zVAD and CPT-zVAD. One hundred micromolar zVAD is used. (*Inset*) Mean velocities of directed motion. $***P < 0.001$ (two-sample *t* test). Error bars indicate SEM. See *SI Appendix*, Table S1 for detailed sample sizes.

To find out when the accelerated directed motion starts to arise during apoptosis, we use the caspase inhibitor zVAD to prevent caspase activation, which is a downstream effect in the apoptotic signaling pathway (28). We find that the accelerated directed motion can still be observed, indicating that it occurs before the caspase activation during the early apoptosis (Fig. 3*B*). Note that the cytosolic ATP concentrations in cisplatin-zVAD– and CPT-zVAD–treated cells remain elevated (*SI Appendix*, Fig. S11). Our observation is consistent with the previous result that ATP responding is an upstream event to the caspase activation (34).

If the accelerated directed motion in the drug-treated apoptotic cells is indeed caused by the elevated ATP level as we propose, then, due to the elevated ATP level, not only the directed motion driven by motor proteins along microtubules is accelerated but also the nondirected diffusive motion in the cytoplasm under randomly fluctuating forces from the stochastic motor activities would increase. It was recently acknowledged that the diffusive motion is not a thermally induced diffusion but results from active processes in the nonequilibrium cytoplasm (16, 17, 38, 39). To test our hypothesis, we measure the diffusive motion of endocytic vesicles in cells, in which the microtubules are fully depolymerized by NOC to eliminate the contribution of directed motion. It was observed that the averaged MSD curve of endocytic vesicles for cisplatin-treated cells increases more quickly than that for the control cells (Fig. 4*A*), and the apparent diffusion rate is accordingly higher (Fig. 4*B*). This demonstrates that the nondirected diffusive motion as an active process is also enhanced by the elevated intracellular ATP level.

It is known that actomyosin contractions are the major source of intracellular forces (40). To investigate how such actomyosin contractions influence the intracellular diffusive motion in early apoptotic cells with elevated ATP level, we treat the cells with 50 μM blebbistatin to inhibit the myosin II motors (41). As a result, the diffusive motion of endocytic vesicles is significantly reduced both in the control and cisplatin-treated cells, with the differences in the MSD curves as well as in the apparent diffusion rates between the two groups being eliminated (Fig. 4). It indicates that the intracellular diffusive motion relies largely on the ATP-dependent actomyosin contractions. Moreover, besides the fluctuating forces, the intracellular diffusive motion is also correlated with intracellular molecule crowding (42); the tracer diffuses faster when the molecule crowding decreases. In our experiments, the similar nondirected diffusive motions in both control and cisplatin-treated cells with no contribution of actomyosin contraction suggests that the intracellular crowding of early apoptosis cells has no obvious change, and thus its possible influence can be eliminated. This further implies that it is the ATP level elevation that is involved in the acceleration of intracellular transport, including both directed and diffusive motions.

Since intracellular transport is the basis for molecule translocation and signal transduction, we therefore investigate the impact of enhanced intracellular transport on the apoptotic process. To do so, we increase the molecule crowding in cells by externally suppressing the cell volume, through osmotic compression. It is known that the reduction of cell volume that results in an increasing intracellular stiffness would affect the directed transport in cells (43, 44). We add 6% 300-Da polyethylene glycol (PEG) to compress the cells, as has been used before. Previous studies have proven that PEG is a biologically compatible polymer, without triggering any immune response

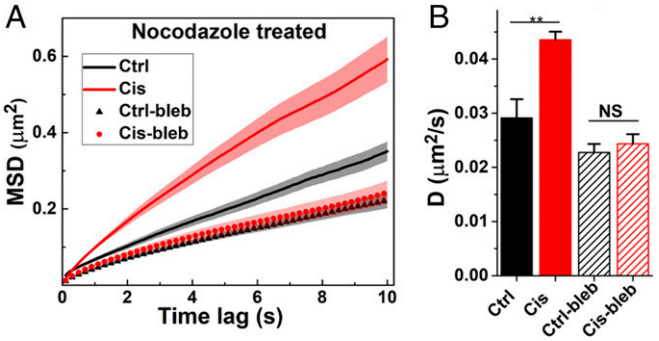

Fig. 4. Acceleration of nondirected diffusive motion in cisplatin-treated cells. To eliminate the contribution of directed motion, 50 μM nocodazole is applied for 30 min to depolymerize the microtubules before the measurements. (*A*) Averaged MSD of all trajectories of QD-labeled vesicles in control cells and that treated with cisplatin, blebbistatin (bleb), and cisplatin–blebbistatin (Cis-bleb). One hundred micromolar blebbistatin is used, which is added to the control and cisplatin-treated cells for 1 h to inhibit the actomyosin contraction. (*B*) Averaged apparent diffusion rates. The apparent diffusion rate for each trajectory is determined by linearly fitting the initial three points of the MSD curve. $^{**}P < 0.01$ (two-sample *t* test). Ctrl, control; NS, not significant. Error bars indicate SEM.

(43, 45). The velocity of the intracellular directed motion is reduced by over 20% for both control and cisplatin groups due to the increased molecule crowding (Fig. 5*A*). The run length and time duration are decreased by 30% and 15%, respectively, for control and cisplatin groups (Fig. 5 *B* and *C*). As a result, the velocity and run length for cells treated with both cisplatin and PEG are close to those of the control group. In other words, we have attenuated the effect of cisplatin on the intracellular transport by adding PEG. Then, we start to check whether the apoptotic progress is affected in this case of no accelerated intracellular transport. For this purpose, all of the cells are stained by the nuclear markers PI and Hoechst (Fig. 5*D*). PI is a fluorescence label for dead cells, whereas Hoechst is for both live and dead cells. Thus, the ratio of cells stained by PI to those stained by Hoechst could indicate the proportion of dead cells. We find that, with the PEG compression, the dead cells under the cisplatin treatment are significantly reduced by 18% and 37% after 12 and 24 h, respectively (Fig. 5*E*). Since ATP is required for cell apoptosis, we check the ATP level in cells treated with both cisplatin and PEG and find that the cytosolic ATP concentration remains elevated and is even higher than that of cells treated by cisplatin alone (*SI Appendix*, Fig. S12). It suggests that although an elevated cytosolic ATP may increase the intracellular transport dynamics, the osmotic compression has a larger negative impact in the experiments. Taken together, the above results indicate that, without the acceleration of intracellular transport, apoptosis could be delayed or impaired even with the cytosolic ATP level being elevated. This suggests strongly that the enhancement of intracellular transport is critical for apoptosis.

Discussion

In this study, by using the SPT method combined with TMRE as the apoptosis indicator for identifying single apoptotic cells under the microscope, we quantify the dynamics of intracellular transport in early apoptotic cells. In contrast with the general concept that apoptosis is programmed with the shutdown of normal physiological activities, we reveal that the intracellular transport, which includes both directed and diffusive motions, is accelerated in the early stage of apoptosis. Intracellular transport is the basis for the translocation and distribution of proteins and organelles in cells and plays key roles in the protein interaction and signaling transduction. In early apoptosis, actually, besides signaling cascades taking place, the organelle mitochondria also undergo fragmentation, aggregation, and rearrangement (46). So the accelerated intracellular transport could offer an essential physical environment to support the initiation and proceeding of physiological apoptosis. Moreover, we examine several factors that are directly involved in the intracellular transport and find that its acceleration likely results from the elevation of cellular ATP concentration in early apoptotic cells. The acceleration of directed motion is observed when caspase is inhibited by zVAD, suggesting that the acceleration arises before the caspase activation.

It is known that intracellular transport is not only correlated with the cellular activities but also affected by the crowded cytoplasmic environment. We notice that the early apoptotic cells we identified have no obvious changes in morphology compared with the control cells, and the apparent diffusion rates are similar in both the early apoptotic and the control cells when the active actomyosin contraction is inhibited. It is thus inferred that the molecule crowding is almost unaltered in early apoptotic cells. Note that late apoptotic cells shrink and bleb, and their physical properties are dramatically changed. As caspase cleaves the major constitutions of cell cytoskeletons as well as motor proteins in late apoptotic cells (4), it is reasonable to believe that the intracellular transport should become less active. Indeed, we observe that the intracellular transport is significantly suppressed in shrinking and blebbing cells (*SI Appendix*, Fig. S7), and almost no directed motion could be detected from the trajectories.

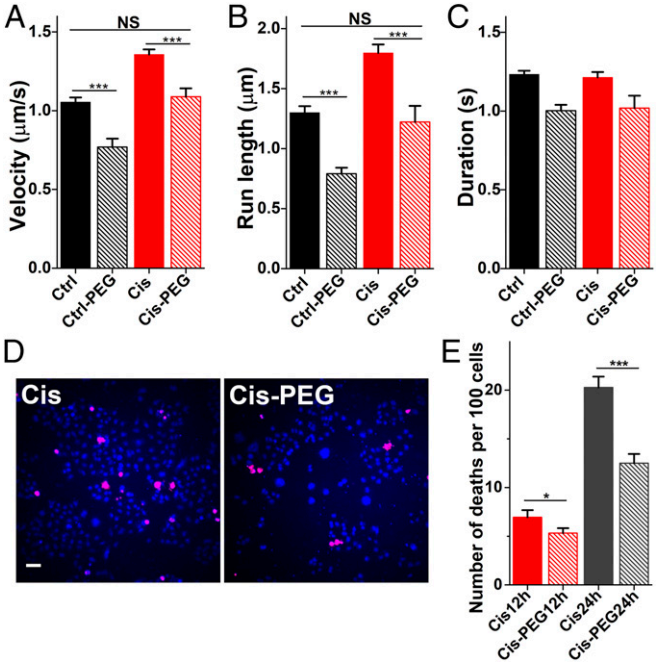

Fig. 5. Number of dead cells under apoptosis stimuli being reduced when intracellular transport dynamics is regulated back to the normal level. (*A*–*C*) Average velocity, duration, and run length of directed motion in control cells and that treated with PEG, cisplatin, and cisplatin plus PEG. To suppress the cell volume by osmotic compression, 6% 300-Da PEG is added to cells along with cisplatin incubation. Osmotic compression by PEG attenuates the degree of accelerated directed motion, and the transport dynamics in cells treated with both cisplatin and PEG is regulated back to the normal level of control cells. See *SI Appendix*, Table S1 for detailed sample sizes. (*D*) Representative images of cells treated with cisplatin and cisplatin plus PEG for 12 h. Cell nuclei are labeled with PI (pink) and Hoechst 33342 (blue). (Scale bar, 60 μm.) (*E*) Numbers of deaths per 100 cells. Total cell numbers: 3,470 (Cis for 12 h), 3,077 (Cis-PEG for 12 h), 2,382 (Cis for 24 h), and 4,220 (Cis-PEG for 24 h). $^{*}P < 0.05$; $^{***}P < 0.001$ (two-sample *t* test). Ctrl, control; NS, not significant. Error bars indicate SEM.

Further studies are required to explore the detailed physical properties of late apoptotic cells.

The most notable finding in the present study is that the apoptotic progress is delayed when the accelerated dynamics of intracellular transport is regulated back to the level of normal cells. We thus reveal a direct correlation between intracellular transport dynamics and cell apoptotic process. It has been shown before that if the ATP level is constrained to the normal level, apoptosis will be abolished (34). Here, we demonstrate that apoptosis is actually determined by the intracellular transport dynamics. The dramatic changes of structures and physiological activities in cells during apoptosis need not only the help of elevated ATP but also the enhanced intracellular transport dynamics. Maintaining rapid intracellular transport is essential for the finely regulated apoptosis of cells. Intracellular transport is known for its high physiological relevance to cellular homeostasis, morphogenesis, and cell motility (38, 47). Recent reports also show that intracellular transport may contribute to the regulation of cellular metabolism (16, 38, 48). Here, we highlight the importance of intracellular dynamics in maintaining physiological functions in cells by illustrating its critical role in determining the apoptotic process with direct evidence. Moreover, accelerated intracellular transport could potentially serve as an indicator for identifying the early apoptotic cells, which is distinct from but also complementary to the TMRE detection under the microscope. This work provides a physical perspective to understand apoptosis in live cells and offers the physical approach of osmotic compaction to control apoptosis. Finally, the observed correlation between enhancement of intracellular transport and apoptosis may be helpful for developing chemotherapy strategies in the treatment of cancer in the future.

Materials and Methods

Full materials and methods are provided in *SI Appendix, SI Materials and Methods*. Briefly, to investigate the intracellular transport, we labeled the transmembrane protein EGFR by EGF and QD consecutively, and imaged the endocytic trafficking of vesicles containing EGFR–EGF-QD complexes in A549 cells under fluorescence microscope. From experimental videos, trajectories of individual endocytic vesicles were extracted, and then segmented into directed and diffusive-like motions by using a user-defined program. We analyzed the dynamic parameters of directed motions for each cell, such as velocity, duration, and run length, and then these dynamic parameters for all cells were averaged to determine the values under different experimental conditions. To induce apoptosis, we treated cells with cisplatin or CPT, and detected their early apoptotic state by using TMRE staining. The cytosolic ATP concentration was quantified using a commercially luminescent ATP detection assay.

ACKNOWLEDGMENTS. We thank M. Guo and H. Y. Wang for helpful discussions. This project was supported by National Natural Science Foundation of China (Grants 11674383, 11774407, and 11874415), Chinese Academy of Sciences Key Research Program of Frontier Sciences (Grant QYZDB-SSW-SLH045), and National Key Research and Development Program (Grant 2016YFA0301500).

1. Fuchs Y, Steller H (2011) Programmed cell death in animal development and disease. *Cell* 147:742–758.
2. Cotter TG (2009) Apoptosis and cancer: The genesis of a research field. *Nat Rev Cancer* 9:501–507.
3. Häcker G (2000) The morphology of apoptosis. *Cell Tissue Res* 301:5–17.
4. Taylor RC, Cullen SP, Martin SJ (2008) Apoptosis: Controlled demolition at the cellular level. *Nat Rev Mol Cell Biol* 9:231–241.
5. Pliss A, Kuzmin AN, Kachynski AV, Prasad PN (2010) Biophotonic probing of macromolecular transformations during apoptosis. *Proc Natl Acad Sci USA* 107:12771–12776.
6. Kang B, Austin LA, El-Sayed MA (2014) Observing real-time molecular event dynamics of apoptosis in living cancer cells using nuclear-targeted plasmonically enhanced Raman nanoprobes. *ACS Nano* 8:4883–4892.
7. Hengartner MO (2000) The biochemistry of apoptosis. *Nature* 407:770–776.
8. Vale RD (2003) The molecular motor toolbox for intracellular transport. *Cell* 112: 467–480.
9. Goldstein JC, et al. (2005) Cytochrome *c* is released in a single step during apoptosis. *Cell Death Differ* 12:453–462.
10. Messam CA, Pittman RN (1998) Asynchrony and commitment to die during apoptosis. *Exp Cell Res* 238:389–398.
11. Manzo C, Garcia-Parajo MF (2015) A review of progress in single particle tracking: From methods to biophysical insights. *Rep Prog Phys* 78:124601.
12. Jayaraman S (2005) Flow cytometric determination of mitochondrial membrane potential changes during apoptosis of T lymphocytic and pancreatic beta cell lines: Comparison of tetramethylrhodamineethylester (TMRE), chloromethyl-X-rosamine (H2-CMX-Ros) and MitoTracker Red 580 (MTR580). *J Immunol Methods* 306:68–79.
13. Sorkin A, Goh LK (2009) Endocytosis and intracellular trafficking of ErbBs. *Exp Cell Res* 315:683–696.
14. Lidke DS, et al. (2004) Quantum dot ligands provide new insights into erbB/HER receptor-mediated signal transduction. *Nat Biotechnol* 22:198–203.
15. Li H, et al. (2012) Effects of paclitaxel on EGFR endocytic trafficking revealed using quantum dot tracking in single cells. *PLoS One* 7:e45465.
16. Guo M, et al. (2014) Probing the stochastic, motor-driven properties of the cytoplasm using force spectrum microscopy. *Cell* 158:822–832.
17. Fakhri N, et al. (2014) High-resolution mapping of intracellular fluctuations using carbon nanotubes. *Science* 344:1031–1035.
18. Brangwynne CP, Koenderink GH, MacKintosh FC, Weitz DA (2008) Cytoplasmic diffusion: Molecular motors mix it up. *J Cell Biol* 183:583–587.
19. Li H, et al. (2015) Mapping intracellular diffusion distribution using single quantum dot tracking: Compartmentalized diffusion defined by endoplasmic reticulum. *J Am Chem Soc* 137:436–444.
20. Ross JL, Ali MY, Warshaw DM (2008) Cargo transport: Molecular motors navigate a complex cytoskeleton. *Curr Opin Cell Biol* 20:41–47.
21. Dasari S, Tchounwou PB (2014) Cisplatin in cancer therapy: Molecular mechanisms of action. *Eur J Pharmacol* 740:364–378.
22. Darzynkiewicz Z, et al. (1997) Cytometry in cell necrobiology: Analysis of apoptosis and accidental cell death (necrosis). *Cytometry* 27:1–20.
23. Lane JD, Allan VJ, Woodman PG (2005) Active relocation of chromatin and endoplasmic reticulum into blebs in late apoptotic cells. *J Cell Sci* 118:4059–4071.
24. Green DR, Reed JC (1998) Mitochondria and apoptosis. *Science* 281:1309–1312.
25. Gonzalez VM, Fuertes MA, Alonso C, Perez JM (2001) Is cisplatin-induced cell death always produced by apoptosis? *Mol Pharmacol* 59:657–663.
26. Zhang LJ, et al. (2008) Inhibition of apoptosis facilitates necrosis induced by cisplatin in gastric cancer cells. *Anticancer Drugs* 19:159–166.
27. Barteneva NS, Ponomarev ED, Tsytsykova A, Armant M, Vorobjev IA (2014) Mitochondrial staining allows robust elimination of apoptotic and damaged cells during cell sorting. *J Histochem Cytochem* 62:265–275.
28. Callus BA, Vaux DL (2007) Caspase inhibitors: Viral, cellular and chemical. *Cell Death Differ* 14:73–78.
29. Jung Y, Lippard SJ (2007) Direct cellular responses to platinum-induced DNA damage. *Chem Rev* 107:1387–1407.
30. Pommier Y (2006) Topoisomerase I inhibitors: Camptothecins and beyond. *Nat Rev Cancer* 6:789–802.
31. Kasparkova J, Marini V, Bursova V, Brabec V (2008) Biophysical studies on the stability of DNA intrastrand cross-links of transplatin. *Biophys J* 95:4361–4371.
32. Eguchi Y, Shimizu S, Tsujimoto Y (1997) Intracellular ATP levels determine cell death fate by apoptosis or necrosis. *Cancer Res* 57:1835–1840.
33. Toba S, Watanabe TM, Yamaguchi-Okimoto L, Toyoshima YY, Higuchi H (2006) Overlapping hand-over-hand mechanism of single molecular motility of cytoplasmic dynein. *Proc Natl Acad Sci USA* 103:5741–5745.
34. Zamaraeva MV, et al. (2005) Cells die with increased cytosolic ATP during apoptosis: A bioluminescence study with intracellular luciferase. *Cell Death Differ* 12:1390–1397.
35. Lieberthal W, Menza SA, Levine JS (1998) Graded ATP depletion can cause necrosis or apoptosis of cultured mouse proximal tubular cells. *Am J Physiol* 274:F315–F327.
36. Waterhouse NJ, et al. (2001) Cytochrome *c* maintains mitochondrial transmembrane potential and ATP generation after outer mitochondrial membrane permeabilization during the apoptotic process. *J Cell Biol* 153:319–328.
37. Ricci JE, et al. (2004) Disruption of mitochondrial function during apoptosis is mediated by caspase cleavage of the p75 subunit of complex I of the electron transport chain. *Cell* 117:773–786.
38. Parry BR, et al. (2014) The bacterial cytoplasm has glass-like properties and is fluidized by metabolic activity. *Cell* 156:183–194.
39. Gupta SK, Guo M (2017) Equilibrium and out-of-equilibrium mechanics of living mammalian cytoplasm. *J Mech Phys Solids* 107:284–293.
40. Koenderink GH, et al. (2009) An active biopolymer network controlled by molecular motors. *Proc Natl Acad Sci USA* 106:15192–15197.
41. Kovács M, Tóth J, Hetényi C, Málnási-Csizmadia A, Sellers JR (2004) Mechanism of blebbistatin inhibition of myosin II. *J Biol Chem* 279:35557–35563.
42. Dix JA, Verkman AS (2008) Crowding effects on diffusion in solutions and cells. *Annu Rev Biophys* 37:247–263.
43. Guo M, et al. (2017) Cell volume change through water efflux impacts cell stiffness and stem cell fate. *Proc Natl Acad Sci USA* 114:E8618–E8627.
44. Hu J, et al. (2017) Size- and speed-dependent mechanical behavior in living mammalian cytoplasm. *Proc Natl Acad Sci USA* 114:9529–9534.
45. Zhou EH, et al. (2009) Universal behavior of the osmotically compressed cell and its analogy to the colloidal glass transition. *Proc Natl Acad Sci USA* 106:10632–10637.
46. Cosentino K, García-Sáez AJ (2014) Mitochondrial alterations in apoptosis. *Chem Phys Lipids* 181:62–75.
47. Sun M, Wartel M, Cascales E, Shaevitz JW, Mignot T (2011) Motor-driven intracellular transport powers bacterial gliding motility. *Proc Natl Acad Sci USA* 108:7559–7564.
48. Li H, et al. (2018) Active transport of cytoophidia in *Schizosaccharomyces pombe*. *FASEB J* 2018:fj201800045RR.